

## Article

# Numerical Simulation of Electric Field Distribution around an Instrumented Total Hip Stem

Ulf Zimmermann <sup>1</sup>, Cathérine Ebner <sup>2</sup>, Yukun Su <sup>2</sup>, Thomas Bender <sup>2</sup>, Yogesh Deepak Bansod <sup>1,\*</sup> ,  
Wolfram Mittelmeier <sup>2</sup>, Rainer Bader <sup>2,3,4</sup> and Ursula van Rienen <sup>1,3,4,\*</sup> 

<sup>1</sup> Institute of General Electrical Engineering, University of Rostock, 18051 Rostock, Germany; ulf.zimmermann@gmx.de

<sup>2</sup> Department of Orthopaedics, University Medicine Rostock, 18057 Rostock, Germany; catherine.ebner@gmx.de (C.E.); yukun.su@uni-rostock.de (Y.S.); PositiverHeld@googlemail.com (T.B.); wolfram.mittelmeier@med.uni-rostock.de (W.M.); rainer.bader@med.uni-rostock.de (R.B.)

<sup>3</sup> Department Ageing of Individuals and Society, University of Rostock, 18051 Rostock, Germany

<sup>4</sup> Department Life, Light & Matter, University of Rostock, 18051 Rostock, Germany

\* Correspondence: yogesh.bansod@uni-rostock.de (Y.D.B.); ursula.van-rienen@uni-rostock.de (U.v.R.); Tel.: +49-381-498-7039 (Y.D.B.); +49-381-498-7070 (U.v.R.)

**Abstract:** Presently, total joint replacement (TJR) is a standard procedure in orthopedic surgery. Adequate osseointegration of the implant components still remains a clinical issue. However, active stimulation of bone tissue to enhance bone ongrowth at the implant surfaces has not been widely investigated so far. For the last several years, invasive electromagnetically induced osseotherapy has been employed in clinical practice, e.g., for the treatment of avascular necrosis, femoral neck fractures, and pseudarthrosis. In the present study, the approach of exploiting the electric stimulation effect was transferred to the field of TJR. Therefore, a commercially available total hip stem was instrumented with an electrode on its surface in order to generate an electric field supporting the regeneration of the surrounding bone tissue. The objective was to conduct numerical simulations validated by experimental investigations as a proof of concept for an instrumented electro-stimulative total hip stem. The results revealed that the calculated electric field around a total hip stem fulfills the requirements to stimulate adjacent bone tissue when using clinically applied electric voltages. The derived numerical and experimental data of electric potentials and corresponding electric fields are encouraging for the implementation of active electrical stimulation in uncemented total hip stems to enhance their osseointegration.

**Keywords:** electrical stimulation; numerical simulation; electric field distribution; experimental validation; osseointegration; total hip replacement (THR)



**Citation:** Zimmermann, U.; Ebner, C.; Su, Y.; Bender, T.; Bansod, Y.D.; Mittelmeier, W.; Bader, R.; van Rienen, U. Numerical Simulation of Electric Field Distribution around an Instrumented Total Hip Stem. *Appl. Sci.* **2021**, *11*, 6677. <https://doi.org/10.3390/app11156677>

Academic Editor: Fabio La Foresta

Received: 13 May 2021

Accepted: 15 July 2021

Published: 21 July 2021

**Publisher's Note:** MDPI stays neutral with regard to jurisdictional claims in published maps and institutional affiliations.



**Copyright:** © 2021 by the authors. Licensee MDPI, Basel, Switzerland. This article is an open access article distributed under the terms and conditions of the Creative Commons Attribution (CC BY) license (<https://creativecommons.org/licenses/by/4.0/>).

## 1. Introduction

Today, total joint replacement (TJR) is a standard procedure in orthopedic surgery. Adequate osseointegration of the implant components is required for their long-term stability within the bone stock. Surface modifications such as bioactive coatings have been developed extensively to stimulate bone ongrowth, and this increases secondary implant stability [1–3]. An alternative for the enhancement of bone ongrowth and stable implant fixation may be the application of electrical stimulation of the adjacent bone tissue. So far, in clinical practice, invasive electromagnetically induced osseotherapy has been used for the stimulation of osseointegration in cases of avascular femoral head necrosis, femoral neck fractures, and pseudarthrosis [4,5]. In this therapeutic approach, based on Kraus and Lechner's [6] work, patients are instrumented with a bipolar induction screw implant such as the Asnis III s-series screw, (Stryker Trauma, Kiel, Germany), which consists of two electrodes and a secondary coil [4]. A primary coil is placed around the patient's leg during treatment, generating a low-frequency magnetic field, which transfers energy inductively to

the electrical stimulation system. Sinusoidal magnetic fields in a frequency range between 12 to 20 Hz and with a voltage of 0.7 V are applied [7]. Therefore, an alternating electric field is provided to the surrounding bone tissue. Usually, the stimulating implant is removed after three months of treatment [4].

A retrospective clinical observation of 53 patients treated with an Asnis III s-series screw showed good postoperative results, i.e., no arthroplasty, no reoperation, and no radiological progress associated with clinical symptoms were observed in 86% of the patients with Steinberg stages I–III after  $33 \pm 20$  months postoperatively [7]. It has been proven by several studies that an electric field of 5–70 V/m is beneficial in order to regenerate bone tissue [6,8–10]. Krüger et al. [11] proved that there was a significant influence of electromagnetic stimulation on the mechanical strength of healing bone at the ovine tibia. In a later animal study, which employed 20 dogs, an increase of 17% new bone formation compared to the control group was seen [12]. The animals were treated with 38 Hz and 0.14 V over 8 weeks with 10 h of stimulation per day. These methods are only used for short-term regeneration of bone tissue over several months and have not been used for long-term electrostimulation of bone cells, bone tissue, or for implant stability, despite the fact that electrical stimulation can also be beneficial for THRs [13–15]. By supporting ongrowth of bone cells at the implant surface and thereby enhancing fixation strength, revision surgery of the THR may be delayed. Furthermore, for revision implants, the stimulation of bone growth is necessary, especially in large bone defects after the removal of primary implant [16]. Therefore, an electrostimulative acetabular revision system with additional individual patient fixations was developed [17,18] as there were no previously existing solutions to actively stimulate the ongrowth of bone cells on total hip stems using electromagnetic fields [19].

In the present study, a commercially available total hip stem was instrumented in order to generate an electric field for enhanced bone regeneration in the surrounding tissue and improved osseointegration of the implant. For this purpose, finite element simulations of the electric field distribution were conducted and validated by experimental investigations in a porcine femur as proof of concept for an instrumented electrostimulative total hip stem.

## 2. Materials and Methods

### 2.1. Modification of a Total Hip Stem

An electrode was integrated into a commercially available straight uncemented total hip stem (HIPSTARV40, Stryker, Duisburg, Germany) made from titanium alloy. For this, the implant was modified by milling a notch into its anterior side. The depth of the notch was 1.5 mm, which was decided based on a static analysis of the implant strength. A width of 3 mm was determined to allow for adequate insulation between the first electrode (Ti6Al4V wire) and the second electrode (total hip stem). The insulating material was made from zirconium oxide ( $ZrO_2$ ), which is a biocompatible ceramic, primarily employed in the field of dentistry.

The Ti6Al4V wire and the insulator were adapted to critical regions of bone ongrowth of straight total hip stems. Clinically, sufficient ongrowth of bone tissue is observed at the lateral and medial parts of the central and distal areas of straight stems [20]. In particular, radiolucent lines are observed at the proximal part, which indicates a lack of bone ongrowth in this implant area. Due to this reason, the notch was positioned in such a manner so as to stimulate in particular the anterior and posterior parts in the proximal and central areas to achieve an additional effect on bone ongrowth by the electric stimulation. The electrodes were supplied by an alternating voltage to allow an electrical field to subsist around the implant. The alternating voltage also facilitated the usage of an inductively coupled system during the clinical application, thus avoiding the need for an internal power source. The energy was transferred by an alternating magnetic field generated by an external coil that was supplied by an external power source.

## 2.2. Reconstruction of the Femur

The geometrical structure of the porcine femur was arranged according to the work in [21]. To this end, CT scans of the femur were created and manually segmented according to their Hounsfield Units (HU) using Amira software (FEI, Burlington, MA, USA) as cortical bone, cancellous bone, and bone marrow (see Figure 1). All tissues were converted to stereolithography (STL) files in American Standard Code for Information Interchange (ASCII) format. Subsequently, these STL files were transferred to the reverse engineering software Geomagic (Geomagic, Stadt, NC, USA) to generate and refine the nonuniform rational B-spline (NURBS) computer-aided design (CAD) models for simulation.

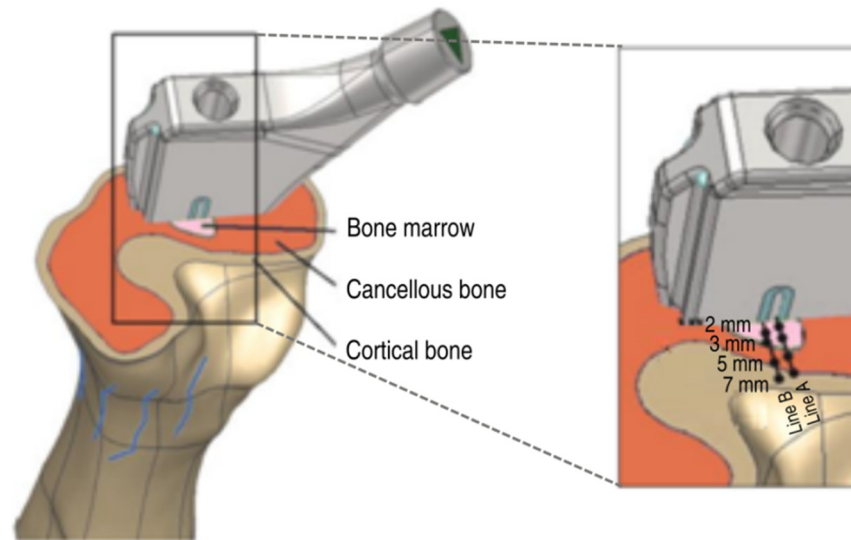


**Figure 1.** CAD model of the porcine femur with the modified total hip stem. The inset displays the measurement points at the cross section of the porcine bone along two lines. The points are allocated on two parallel lines at 2, 3, 5, and 7 mm from the first electrode (line A) and from the interface between insulator and implant (line B).

## 2.3. Numerical Simulations

The simulations were performed using commercial software SIMULIA CST Studio Suite (Dassault Systèmes, [www.3ds.com/simulia](http://www.3ds.com/simulia), accessed on 10 May 2021), and the electric field within the femur model was computed. Here, the specific solver used was based on the Finite Integration Technique (FIT). The assembly of the computational domain was based on the reconstruction of the femur and the CAD model of the hip stem. Both were fitted into the numerical model, with the coordinates being taken by the coordinate measuring arm of the experimental setup for the sake of better comparison of computed and measured results.

The dielectric properties of the different tissues (bone marrow, cancellous bone, and cortical bone) were defined using the parameters from Gabriel et al. [22] and Hasgall et al. [23] as provided for human bone as no data were available for the porcine bone. It had to be assumed, though, that the dielectric properties of the adolescent porcine bone tissues differ from adult human bone tissues. This simulation is referred to as case study 1. Because of the almost insulating properties of the bone marrow when using parameters from Gabriel et al. [22], a second simulation was performed using the conductivity of the cancellous bone within the domain of the bone marrow. This simulation is referred to as case study 2. Furthermore, case study 3 was performed using the parameters from Hasgall et al. [23] but with red bone marrow. As the electric conductivity of titanium is considerably higher than that of the biological tissue, a Perfect Electric Conductor (PEC) could be used rather than including titanium into the computational domain, which reduced the computational effort. Conversely, the insulator has a considerably lower conductivity compared to the biological tissue. Due to this reason, it was defined as a perfect electric insulator (a vacuum).

The electric double layer, which exists at the interface between electrodes and organic tissue, as well as between the implant surface and organic tissue, was characterized by its impedance  $Z$  based on the approximate formula below using measured data of its surface  $A$  along with the impedance  $Z_{Sample}$  measured for a sample electrode with the surface  $A_{Sample}$ .

$$Z \approx \frac{A_{Sample}}{A} Z_{Sample}. \quad (1)$$

Using this approximation, an impedance of 3 k $\Omega$  at the electrode and 120  $\Omega$  at the hip stem was calculated. After the first simulation, the determination of the impedance of the bone sample got possible. For the dielectric tissue parameters as proposed by Gabriel et al. [22], the resultant impedance was 13.25 k $\Omega$ . To consider the effects of the double layer, its impedances were considered in a serial connection with the impedance of the organic tissue. Using the equation

$$\frac{U}{U_{total}} = \frac{Z}{Z_{total}}, \quad (2)$$

the boundary conditions for the simulation were reset to 0.044 V instead of 0.000 V at the hip stem and 4.900 V instead of 6.000 V at the electrode.

The problem was discretized on a hexahedral mesh in conjunction with the Enhanced Fast Perfect Boundary Approximation (EFPBA), which provided an accurate geometrical approximation of the continuous structure. In particular, the mesh around the electrode and the insulator was enhanced to ensure an optimal resolution in the area of interest. The mesh around the readout locations was also densified to avoid interpolation errors. During the first simulations, the adaptive mesh refinement was used to improve the hexahedral mesh automatically. As a result of the convergence study, the final mesh consisted of approximately 9.55 million mesh cells.

Due to the relatively low applied frequency, the capacitive properties of the biological tissues could be neglected. For this reason, the stationary current solver of CST EM STUDIO<sup>®</sup> was used. Prior tests revealed that the error, created by the simplification, was below 0.5% compared to the quasistatic solutions, while computation time was reduced drastically. The computation time for a solver accuracy of  $1 \cdot 10^{-9}$  of the linear solver was less than 10 min when a workstation computer ( $4 \times 2.53$  GHz, 12 GB RAM) was used. The electric fields caused by the voltage of the experiment were considerably higher than the proposed maximum field strength of 70 V/m. This was due to the supply voltage of 6 V during the experiment that was selected to simplify the measurement and to minimize measurement errors. In order to compare the simulated distribution of the electric field during the experiment with the proposed electric field during the clinical situation, further simulations were performed using the proposed supply voltage of 0.2 V.

#### 2.4. Experimental Setup

To prove the numerical simulation's accuracy, a validation experiment was set up according to the clinical application. Therefore, the instrumented total hip stem was inserted into a porcine femur. For this, the femoral head was cut and a borehole ( $\varnothing$  12 mm) was drilled along the axis of the femur. The bone stock was carefully prepared with rasps. Using a hammer, the total hip stem was inserted into a press-fit fixation in order to allow close contact with the surrounding bone tissue. The wire that connected the first electrode was led through the porcine femur to the power supply. The total hip stem was also connected to the power supply (Agilent 33220A, Agilent Technologies Inc., Colorado Springs, CO, USA).

A three-dimensional (3D) coordinate measuring arm (MicroScribe G2x, Solution Technologies, Oella, MD, USA) was used to determine the coordinates of the readout locations, which were maintained as consistent in the numerical simulations. The function generator supplied an alternating field (20 Hz, 6 V). Before the total hip stem was implanted into the bone, the root mean square (RMS) voltage on the surface of the hip stem was measured using a multimeter. This value was used as a boundary value on the hip stem in

the numerical simulation in order to compare the data with the experiment. The potential on the surface of the cross section of the bone was measured at different points along two lines perpendicular to the electrode and to the interface between the insulator and the stem. The points measured were at distances of 2, 3, 5, and 7 mm (Figure 1) along these two lines.

A raster of 10 different points (readout locations) at a distance of 10 mm was marked at the surface of the frontal femur (Figure 2). The electric potential was measured for all points of the raster at approximately 5 mm and 8 mm depth into the bone. This measurement was performed in triplicate. During measurements, the bone tissue was rehydrated with an NaCl solution (conductivity of about 1.5 S/m) to minimize the influence of dehydration of the specimen.

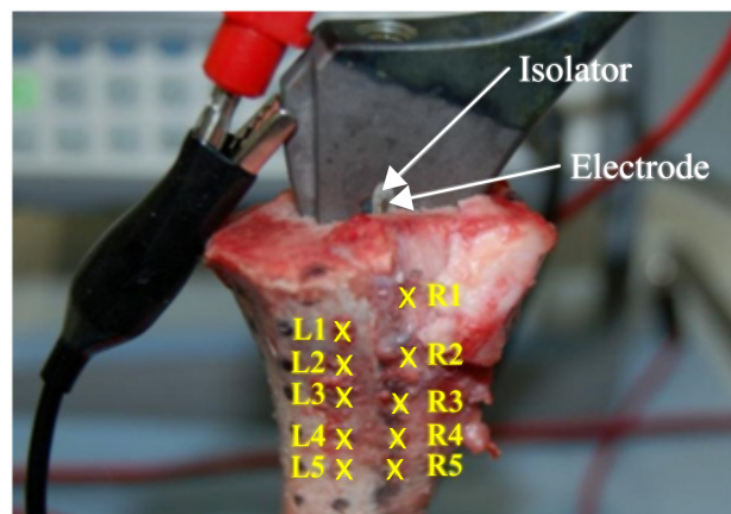


**Figure 2.** Experimental setup with the connected hip stem. A raster of 10 different readout locations at the surface of the porcine femur was used.

### 3. Results

The results of the measurements on the cross section of the porcine femur perpendicular to the first electrode and the interface between the insulator and the implant have been shown in Table 1. As in a homogeneous medium the electric potential varies inversely proportional with the distance from the electrode, it could be roughly expected that measurements on line B starting from the interface between the implant and the insulator resulted in smaller values of the potential than measurements on line A starting from the first electrode. This holds true except for the measured values at a distance of 7 mm. The distinctive distribution of the electric potential demonstrates that the highest values of 1.68 V, 1.25 V, and 1.17 V (case studies 1–3) were obtained on line A. The investigation of the potential at the cross section of the bone resulted in a decay of 78% on line A (2–7 mm) and 72% on line B. In case study 1, the decay amounted to 68% along line A. For case study 2, it was 53% and for case study 3, it was 46%. In general, case study 3 came closest to the measured values, with deviations in the range of 0.01 V–0.25 V. Regarding the differences in measured and simulated potential values, one should keep in mind that there are several error sources both in measurements as well as in the numerical simulations. The most important error source in the simulations has to be attributed to the lack of data on dielectric tissue properties for porcine bone which is why the data from human bone needed to be taken. Additionally, there is rather high uncertainty in general in dielectric tissue properties in the low-frequency spectrum.

**Table 1.** Electric potential measured on the cross-section of the bone perpendicular to the first electrode and the interface between implant and insulator.

	Distance to the Implant (mm)	Potential (V)			
		Experimental	Simulation		
			Case Study 1 [22]	Case Study 2 [22]	Case Study 3 [24]
Line A starting from the first electrode	2	0.99	1.68	1.25	1.17
	4	0.76	1.24	0.95	0.87
	5	0.49	0.57	0.73	0.63
	7	0.22	0.54	0.59	0.47
Line B starting from the implant-insulator interface	2	0.81	1.19	0.90	0.80
	4	0.52	1.10	0.78	0.69
	5	0.42	0.65	0.63	0.53
	7	0.23	0.53	0.54	0.43

The distribution of the electric field strength and the electric potential in the numerical simulation shows a strong stimulation capacity of the surrounding bone tissue (Figures 3 and 4). The implant surface is also stimulated. When the tissue properties from Gabriel et al. [22] for yellow bone marrow were used, its insulating effect on the electric field distribution became evident (see Figure 3a). In the case of using higher conductivity as of red bone marrow [23], the electric field reached a larger area of the surrounding bone and was more evenly distributed (see Figure 3b).

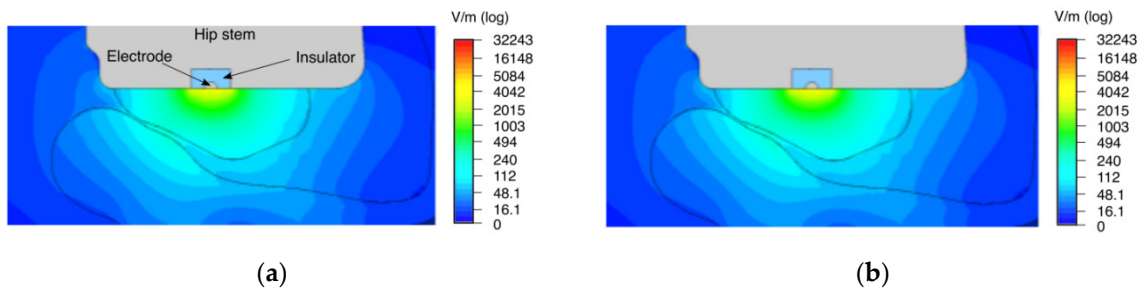


**Figure 3.** Distribution of the electric field strength in the transversal plane of the porcine femur. Conductivity values of (a) yellow bone marrow (case study 1) [22] and (b) red bone marrow (case study 3) [23] have been employed here.

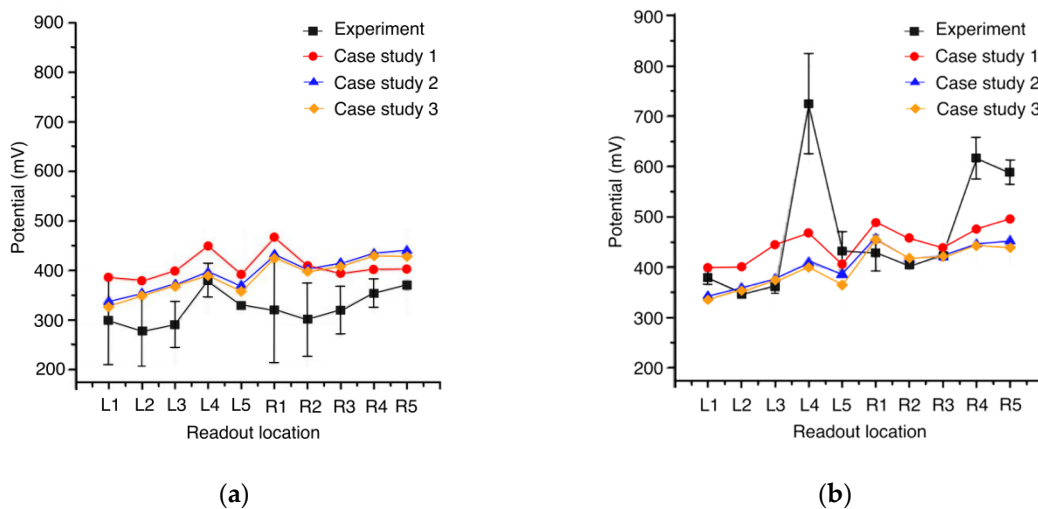


**Figure 4.** Measured and simulated electric potential values. Values are shown on readout locations L1–L5 of the raster followed by readout locations R1–R5 of the raster, each at a depth of (a) 5 mm and (b) 8 mm within the stimulated porcine femur.

In case studies 2 and 3, the electric potential at the raster displays the same trend due to the similar potential values of red bone marrow and cancellous bone (Figure 4). Moreover, for both simulation studies, the potential at the left side of the raster, i.e., readout locations L1–L5, is closer to the experimental values compared to case study 1. The highest experimental value for the electric potential was measured at readout location L4 and showed high standard deviation (Figure 4b).

According to the measurements at the cross section of the porcine femur, case study 3 (Figure 5) showed the overall best agreement with the experiment. As displayed in Figure 4a, deviations were observed in the range of 1 to 25% at 5 mm depth between case study 3 and the experimental results. At 8 mm depth, deviations were within 1–41%, except for readout location L4, as obvious from Figure 4b. In the sequel, case study 3 was compared to the simulation with 0.2 V (Figure 5b) supply under clinical conditions because of the overall better approximation compared to the other two case studies.

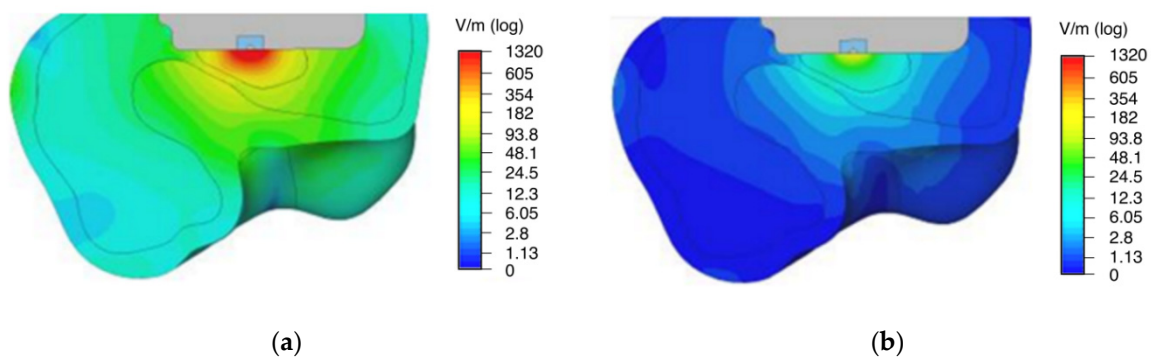


**Figure 5.** Electric field distribution obtained for case study 3. A voltage of (a) 6.0 V and (b) 0.2 V was applied at 20 Hz, representing clinical conditions.

#### 4. Discussion

In the present study, we investigated the general feasibility of an electrostimulative uncemented total hip stem. The bone, being in close proximity to the implant, provides most of the mechanical stability. For this reason, the area close to the implant is of highest interest and thus the electrical stimulation can be limited to the closest bone on both sides of the implant. Therefore, the electric potential values at the cross section of a porcine femur and along a defined raster along the porcine femur defined at depths of 5 mm and 8 mm into the bone were measured in an experiment and compared to results from three different numerical simulation scenarios. Based on two different conductivity values for bone marrow, three case studies were performed in order to discover the most precise model to replicate the physiological behavior of the bone. In the first simulation scenario (case study 1), yellow bone marrow was simulated with low conductivity [22]. The second simulation scenario (case study 2) excluded bone marrow by replacing it with cancellous bone, and the third simulation scenario (case study 3) worked with data from Hasgall et al. [23], including red bone marrow. In our survey, it was found that case study 3 represented the best approximation to the validation experiment performed. In this case study [24], the predicted potential (see Table 1) was in good agreement with our experimentally measured values at the cross section of the porcine femur, thus supporting our assumption of electric field distribution with the bone tissue. In this context, a closer investigation of the influence of tissue conductivity on the electric field distribution of the electrostimulative total hip revision system has been performed [24].

As the electric properties of biological tissues behave linearly at a fixed frequency, the factor used to decrease the stimulation voltage can also be used to decrease the electric field. During the experiment, the primary goal was to generate a high potential to achieve a value several magnitudes above the error tolerance of the multimeter. This resulted in high gradients of the potential and the electric field as can be observed in Figure 5a.

For clinical use, the electric fields for bone regeneration are required to be between 5 and 70 V/m [6]. In this first approach, a voltage of 0.2 V was selected to achieve the desired electric field strengths. The yellow and red area in Figure 5a can be considered over-stimulated ( $>70$  V/m). This area had to be minimized, which means that the voltage had to be reduced. In contrast, the dark blue area in Figure 5b was not stimulated sufficiently ( $<5$  V/m), and to minimize this area, the stimulation voltage had to be increased. Both these contradictory goals can be accomplished without changes in the voltage by slightly increasing the width of the insulator [25].

A limitation of our experiments was given by the high standard deviations of the measured potential. These were likely due to the drying out and rehydration processes performed during measurements. Another reason for the deviations is the use of bone tissue from adolescent pig, which does not have the same dielectric properties as an adult human bone tissue [26]. Figures 4 and 5 show that apart from readout location L4 at 8 mm depth, the values of the simulation were close to the measured potential in the experiment. The outlier behavior of readout location L4, which had a 99% (depth 8 mm) deviation from simulations 2 and 3, necessitates an investigation of the boundary conditions of the experiment. Due to this reason, the relevant CT scan at the height of L4 was examined in detail. The dark areas within the cancellous bone and marrow are fluids, which increases the conductivity significantly at these locations. As the CT scan was performed prior to the implantation of the stem, the position of these fluids may have changed during the implantation. The fluids may have also affected the potentials at readout locations L3 and L5. This effect was not confirmed in measurements at readout locations near the boundary between cortical and cancellous bone at a depth of 5 mm.

A further limitation of the study was the model of the electric double layer, used for the simulation. This is a simplification of the passivation layer of the titanium. The relatively high voltage of 6 V compared to the desired clinical application was induced directly and was used because of a simplified measurement setup. Furthermore, the stationary current solver of CST EM STUDIO<sup>®</sup> was used to calculate the electric potential and electric field strength in all tissues. In clinical studies, a frequency of 20 Hz is used. Analytically, the maximum error using the stationary current solver instead of the electro-quasistatic solver is below 6%. This is due to the low stimulation frequency. Earlier studies comparing the stationary solver with the electro-quasistatic solver showed deviations below 0.5%. Higher deviations are possible due to the uncertainty and minor local changes in the dielectric tissue properties. Therefore, the stationary current solver was used.

An additional limitation was the conductivity values used for this work. In other studies [22,27], bovine, canine, and human tissues were considered, which showed different tissue properties [23]. These variations may also be the reason for deviations in the generated electric fields. Other simplifications of the model were the use of perfect electric conductors instead of titanium and the use of perfect insulators instead of ZrO<sub>2</sub>. As the electric conductivity of the bone was within a magnitude of 0.01 S/m, the error introduced by this idealization may well be assumed to be insignificant. The coordinates measured with the coordinate-measuring arm were another source of error as the measurement device offers limited accuracy and because some of the coordinates were measured on top of moderately soft tissue, which could have been neglected during the segmentation process. The absolute coordinates were used to define the position of the bone and implant for the numerical model. However, the maximal deviation of these measurement points and the supposed point on the surface of the CAD model was 0.27 mm.

In future studies, the size of the insulator and electrode as well as the number of electrodes should be optimized numerically to achieve electric field strengths between 5 and 70 V/m, without affecting the mechanical requirements of the total hip stem. In comparison to the electromagnetic stimulation in osseotherapy [6], the electrodes at the implant can be assembled horizontally. The arrangement differs from the systems currently used in osseotherapy, as it employs parallel electrodes [7]. The application of only electric

fields and electric potentials could be realized by the use of an intelligent implant that provides the power supply.

## 5. Conclusions

The numerical and experimental results after integration of an electrode into the frontal side of a total hip stem demonstrate that the electric potentials and corresponding electric fields can be used as a basis to develop electrically stimulating endoprosthetic implants. Our numerical and experimental results demonstrate the possibility to integrate electrodes into a total hip stem for application of electric potentials and corresponding electric fields to the adjacent bone stock. In further research, this active electrostimulative concept should be analyzed in a living biological environment, i.e., enhanced osseointegration of the electrostimulating implant has to be approved in animal testings. Based on this work, future research studies may be conducted to optimize the electrostimulative parameters such as electric field distribution and to realize power supply of electrostimulating implants in the future.

**Author Contributions:** Conceptualization, U.Z., Y.S., R.B. and U.v.R.; methodology, U.Z., Y.S., R.B. and U.v.R.; software, U.Z.; validation, U.Z. and Y.S.; formal analysis, U.Z. and Y.S.; investigation, U.Z., C.E. and Y.S.; resources, R.B. and U.v.R.; data curation, U.Z. and Y.S.; writing—original draft preparation, U.Z., C.E., Y.S., T.B. and Y.D.B.; writing—review and editing, W.M., R.B. and U.v.R.; visualization, U.Z., C.E., Y.S. and Y.D.B.; supervision, R.B. and U.v.R.; project administration, R.B. and U.v.R.; funding acquisition, R.B. and U.v.R. All authors have read and agreed to the published version of the manuscript.

**Funding:** Funded by the Deutsche Forschungsgemeinschaft (DFG, German Research Foundation)—SFB 1270/1—299150580 and GRK 1505.

**Informed Consent Statement:** Not applicable.

**Acknowledgments:** We thank the Deutsche Forschungsgemeinschaft (DFG) for financial support (Research Training Group GRK 1505 welisa, Collaborative Research Centre SFB 1270/1 ELAINE—299150580), and DCM GmbH, Rostock, Germany for technical support in insulation of the electrodes.

**Conflicts of Interest:** The authors declare no conflict of interest.

## References

1. Capello, W.N.; D'antonio, J.A.; Feinberg, J.R.; Manley, M.T. Ten-year results with hydroxyapatite-coated total hip femoral components in patients less than fifty years old. *J. Bone Jt. Surg. Amer. Vol.* **2003**, *85*, 885–889. [[CrossRef](#)]
2. Oosterbos, C.; Rahmy, A.; Tonino, A. Hydroxyapatite coated hip prosthesis followed up for 5 years. *Int. Orthop.* **2001**, *25*, 17–21. [[CrossRef](#)]
3. Ruther, C.; Gabler, C.; Ewald, H.; Ellenrieder, M.; Haenle, M.; Lindner, T.; Mittelmeier, W.; Bader, R.; Kluess, D. In vivo monitoring of implant osseointegration in a rabbit model using acoustic sound analysis. *J. Orthop. Res.* **2014**, *32*, 606–612. [[CrossRef](#)] [[PubMed](#)]
4. Mittelmeier, W.; Lehner, S.; Kraus, W.; Matter, H.P.; Gerdesmeyer, L.; Steinhauser, E. BISS: Concept and biomechanical investigations of a new screw system for electromagnetically induced internal osteostimulation. *Arch. Orthop. Trauma Surg.* **2004**, *124*, 86–91. [[CrossRef](#)] [[PubMed](#)]
5. Bassett, C.A.L.; Pawluk, R.J.; Pilla, A.A. Acceleration of fracture repair by electromagnetic fields. A surgically noninvasive method. *Ann. N. Y. Acad. Sci.* **1974**, *238*, 242–262. [[CrossRef](#)] [[PubMed](#)]
6. Kraus, W. Magnetic field therapy and magnetically induced electrostimulation in orthopedics. *Orthopäde* **1984**, *13*, 78.
7. Ellenrieder, M.; Tischer, T.; Kreuz, P.; Fröhlich, S.; Fritsche, A.; Mittelmeier, W. Arthroskopisch gestützte Behandlung der aseptischen Hüftkopfnekrose. *Oper. Orthop. Traumatol.* **2013**, *25*, 85–94. [[CrossRef](#)]
8. Soda, A.; Ikehara, T.; Kinouchi, Y.; Yoshizaki, K. Effect of exposure to an extremely low frequency-electromagnetic field on the cellular collagen with respect to signaling pathways in osteoblast-like cells. *J. Med. Investig.* **2008**, *55*, 267–278. [[CrossRef](#)]
9. Aaron, R.K.; Ciombor, D.M.; Simon, B.J. Treatment of Nonunions with Electric and Electromagnetic Fields. *Clin. Orthop. Relat. Res.* **2004**, *419*, 21–29. [[CrossRef](#)]
10. Su, Y.; Souffrant, R.; Kluess, D.; Ellenrieder, M.; Mittelmeier, W.; van Rienen, U.; Bader, R. Evaluation of electric field distribution in electromagnetic stimulation of human femoral head. *Bioelectromagnetics* **2014**, *35*, 547–558. [[CrossRef](#)]
11. Krüger, T.; Hein, W.; Plitz, W. Einfluss der magnetisch induzierten Elektrostimulation (MIES) auf die Kallusfestigkeit nach Distraction der Schaftstibia. *Osteologie* **2000**, *9*, 157–164.

12. Schmit-Neuerburg, K.-P. Indikation und klinische Ergebnisse der magnetfeldinduzierten Wechselstromstimulation verzögert heilender Frakturen und Pseudarthrosen. *Trauma Berufskrankh.* **2001**, *3*, S66–S72. [[CrossRef](#)]
13. Brighton, C.T.; Wang, W.; Seldes, R.; Zhang, G.; Pollack, S.R. Signal Transduction in Electrically Stimulated Bone Cells. *J. Bone Jt. Surg. Am. Vol.* **2001**, *83*, 1514–1523. [[CrossRef](#)]
14. Devet, T.; Jhirad, A.; Pravato, L.; Wohl, G.R. Bone Bioelectricity and Bone-Cell Response to Electrical Stimulation: A Review. *Crit. Rev. Biomed. Eng.* **2021**, *49*, 1–19. [[CrossRef](#)]
15. Dauben, T.J.; Ziebart, J.; Bender, T.; Zaatreh, S.; Kreikemeyer, B.; Bader, R. A Novel In Vitro System for Comparative Analyses of Bone Cells and Bacteria under Electrical Stimulation. *BioMed Res. Int.* **2016**, *2016*, 1–12. [[CrossRef](#)]
16. Paprosky, W.G.; Magnus, R.E. Principles of Bone Grafting in Revision Total Hip Arthroplasty. *Clin. Orthop. Relat. Res.* **1994**, 147–155. [[CrossRef](#)]
17. Kluess, D.; Souffrant, R.; Bader, R.; van Rienen, U.; Ewald, H.; Mittelmeier, W. A New Concept of an Electrostimulative Acetabular Revision System with Patient Individual Additional Fixation. In Proceedings of the 4th European Conference of the International Federation for Medical and Biological Engineering ECIFMBE 2008, Antwerp, Belgium, 23–27 November 2008; Springer: Berlin/Heidelberg, Germany, 2009; pp. 1847–1850. [[CrossRef](#)]
18. Potratz, C.; Kluess, D.; Ewald, H.; van Rienen, U. Multiobjective Optimization of an Electrostimulative Acetabular Revision System. *IEEE Trans. Biomed. Eng.* **2009**, *57*, 460–468. [[CrossRef](#)] [[PubMed](#)]
19. Latham, W.; Lau, J.T. Bone Stimulation. *Tech. Orthop.* **2011**, *26*, 14–21. [[CrossRef](#)]
20. Suckel, A.; Müller, O.; Herberths, T.; Wulker, N. Changes in Chopart joint load following tibiotalar arthrodesis: In vitro analysis of 8 cadaver specimen in a dynamic model. *BMC Musculoskelet. Disord.* **2007**, *8*, 80. [[CrossRef](#)] [[PubMed](#)]
21. Kluess, D.; Souffrant, R.; Mittelmeier, W.; Wree, A.; Schmitz, K.-P.; Bader, R. A convenient approach for finite-element-analyses of orthopaedic implants in bone contact: Modeling and experimental validation. *Comput. Methods Programs Biomed.* **2009**, *95*, 23–30. [[CrossRef](#)] [[PubMed](#)]
22. Gabriel, S.; Lau, R.W.; Gabriel, C. The dielectric properties of biological tissues: II. Measurements in the frequency range 10 Hz to 20 GHz. *Phys. Med. Biol.* **1996**, *41*, 2251–2269. [[CrossRef](#)] [[PubMed](#)]
23. Hasgall, P.; Neufeld, E.; Gosselin, M.; Klingensböck, A.; Kuster, N. *IT'IS Database for Thermal and Electromagnetic Parameters of Biological Tissues*; Version 2.5; The Foundation for Research on Information Technologies in Society (IT'IS): Zurich, Switzerland, 2014.
24. Ewald, H.; Bader, R.; Kluess, D.; Souffrant, R.; Potratz, C.; van Rienen, U.; Mittelmeier, W. Untersuchungen der elektrischen und dielektrischen Eigenschaften von Hüftknochen für den Einsatz elektrostimulierender Implantate. In Proceedings of the 5th Symposium on Automatic Control, Genova, Italy, 18–19 September 2008; pp. 1847–1850.
25. Zimmermann, U.; Van Rienen, U. On the optimization of the hip stem for an electrostimulative hip revision system. In Proceedings of the 2014 XXXIth URSI General Assembly and Scientific Symposium (URSI GASS), Beijing, China, 16–23 August 2014; Institute of Electrical and Electronics Engineers (IEEE): Piscataway, NJ, USA, 2014; pp. 1–4.
26. Schmidt, C.; Zimmermann, U.; Van Rienen, U. Uncertainty quantification of the optimal stimulation area in an electro-stimulative hip revision system. In Proceedings of the 36th Annual International Conference of the IEEE Engineering in Medicine and Biology Society, Chicago, IL, USA, 26–30 August 2014; Institute of Electrical and Electronics Engineers (IEEE): Piscataway, NJ, USA, 2014; Volume 2014, pp. 824–827.
27. Gabriel, S.; Lau, R.W.; Gabriel, C. The dielectric properties of biological tissues: III. Parametric models for the dielectric spectrum of tissues. *Phys. Med. Biol.* **1996**, *41*, 2271–2293. [[CrossRef](#)] [[PubMed](#)]